2011 American Control Conference
on O'Farrell Street, San Francisco, CA, USA
June 29 - July 01, 2011

A multiscale stochastic approach for phase screens synthesis

Alessandro Beghi, Angelo Cenedese, and Andrea Masiero

Abstract— **Simulating the turbulence effect on ground telescope observations is of fundamental importance for the design and test of suitable control algorithms for adaptive optics systems. In this paper we propose a multiscale approach for efficiently synthesizing turbulent phases at very high resolutions: First, the turbulence is simulated at low resolution taking advantage of a previously developed method for generating phase screens, [2]. Then, high resolution phase screens are obtained as the output of a multiscale linear stochastic system. The multiscale approach significantly improves the computational efficiency of turbulence simulation with respect to recently developed methods [1],[2],[8]. Furthermore, the proposed procedure ensures good accuracy in reproducing the statistical characteristics of the turbulent phase.**

I. INTRODUCTION

Motivated by the increasing importance of adaptive optics (AO) systems for improving the real resolution of large ground telescopes, in this paper we address the problem of turbulence simulation to provide a test bed for the design of control strategies for AO systems.

The presence of wind and local temperature changes cause rapid changes in the atmosphere's refraction index, [14]. Thus, when the wavefront signal arriving from a star object enters the terrestrial atmosphere it is distorted proportionally to the length of its optic path, and depending on the encountered refraction index. Consequently, the atmospheric turbulence effect is mainly to delay the light beams of different phases. Therefore, the flat wavefront surface of a light beam arriving from a star is no longer flat when it is detected on the telescope pupil: This significantly reduces the real resolution of the telescope.

The atmospheric turbulence effect can be modeled as a randomly changing phase delay added to the light beams phase. Such delay, which we will also call turbulent phase, can be statistically characterized as a zero-mean second order random process. Similarly, a phase screen can be defined as the set of phase values which affect the light beams wavefront arriving on the telescope.

Commonly used methods for the turbulent phase simulation are based on the fast Fourier transform (FFT). On the positive side, such methods allow to quickly generate turbulence samples which perfectly match the theoretical turbulent phase statistical characteristics. On the other hand, since they generate all the samples together, they can be used only for synthesizing finite dimensional phase screens.

A.Beghi and A.Masiero are with the Dipartimento di Ingegneria dell'Informazione, Università di Padova, via Gradenigo 6/B, 35131 Padova, Italy {beghi,masiero}@dei.unipd.it

A.Cenedese is with the Dipartimento di Tecnica e Gestione dei Sistemi Industriali, Università di Padova, Stradella San Nicola 3, 36100 Vicenza, Italy angelo.cenedese@unipd.it

The interest in studying the performances of AO control algorithms in long simulations led to different approaches for simulating the turbulence: Recently proposed procedures, [1],[2],[8], exploit a suitably defined linear dynamic system to model the spatio-temporal dynamic of the turbulent phase along the wind direction. Then, such dynamic system, driven by white noise, is used to produce, possibly infinitely long, sequences of phase screens samples.

In this paper we propose a new approach which combines the method described above, [1],[2],[8], with a multiscale stochastic model: The first is used to compute a low resolution version of the phase screen, while the latter provides an efficient way to obtain high resolution phase screens starting from the results of the first. The overall algorithm is computationally more efficient than those in [1],[2],[8], and, as shown in Section V, it accurately reproduces the desired turbulence statistical characteristics.

The multiscale approach proposed here, is similar to already considered multiscale models [11],[3],[5],[9],[7]: As in [5] we a priori fix a multiresolution representation of the turbulence (e.g. a wavelet decomposition, [6],[12]) and similarly to [7] we exploit local spatial predictions to reduce the spatial correlation of the considered signal. However, differently from previously considered approaches, the error process obtained after prediction is modeled like a moving average process, leading to an efficient way for matching the theoretical turbulence statistical characteristics at each scale of the representation.

The contribution of this paper is twofold: First, the integration of spatio-temporal models [1],[2],[8] with a multiscale stochastic model, which allows to more efficiently synthesize phase screens. Second, the proposed multiscale approach shall be of some interest in the multiscale realization theory: Developments on this aspect are still under investigation.

The paper is organized as follows: Section II introduces the turbulence spatio-temporal statistical characteristics. In Section III we introduce a multiscale representation of the turbulent phase. Then, in Section IV we present the main results, proposing a new multiscale stochastic model of the atmospheric turbulence. Finally, in Section V we discuss the results of some simulations.

II. TURBULENT PHASE CHARACTERIZATION

The turbulent phase is assumed to be zero-mean stationary and spatially homogeneous. Let $\mathbf{u}$ and $\mathbf{v}$ be two unit vectors indicating two orthogonal spatial directions, as in Fig. 1, and let $\phi(u, v, t)$ be the value of the turbulent phase on the point (u, v) at time t on the telescope aperture plane, where u and v are the coordinates of the point along $\mathbf{u}$ and $\mathbf{v}$. Then, the

978-1-4577-0079-8/11/$26.00 ©2011 AACC

covariance between two values of the turbulence, $\phi(u,v,t)$ and $\phi(u',v',t)$, depends only on the distance, r, between the two points: $C_\phi(r) = \mathbf{E}[\phi(u,v,t)\phi(u',v',t)], \forall(u,v,u',v')$, such that $r = \sqrt{(u-u')^2+(v-v')^2}$.

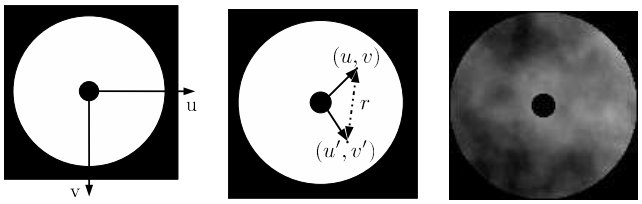

(a) (b) (c)

Fig. 1. (a) Coordinates on the telescope image domain. (b) Two points, (u,v) and (u',v'), separated by a distance r on the telescope aperture plane. (c) An example of phase screen.

According to the Von Karman theory, the shape of the spatial covariance function, $C_\phi(\cdot)$, is completely characterized by the values of two physical parameters, r_0, the Fried parameter, and L_0, the outer scale ([14], [4]):

$$C_\phi(r) = \left(\frac{L_0}{r_0}\right)^{5/3} \frac{\eta}{2} \left(\frac{2\pi r}{L_0}\right)^{5/6} K_{5/6}\left(\frac{2\pi r}{L_0}\right), \quad (1)$$

where $K_\cdot(\cdot)$ is the MacDonald function (modified Bessel function of the third type), and η is a constant.

Furthermore, the turbulent phase is supposed to be normally distributed [13], hence the second order statistics are sufficient to completely describe its statistical properties.

From a temporal point of view, the turbulence is typically modeled as a (linear) superposition of a finite number l of independent layers, moving at different altitudes, with different energies and velocities. A commonly agreed assumption considers that each layer translates in front of the telescope pupil with constant velocity $\boldsymbol{v}_i$ (Taylor approximation [14]).

III. MULTISCALE APPROACH FOR TURBULENT PHASE SIMULATION

Since the layers are independent here we consider the problem of simulating a single layer. Furthermore, we assume that the wind direction associated to the considered layer is parallel to the $\mathbf{v}$ vector, i.e. $\boldsymbol{v}_i = v_{i,\mathbf{v}}\mathbf{v}$, $v_{i,\mathbf{v}} \neq 0$.

Without loss of generality, we assume the phase screen (Fig. 1(c)) to be represented as an $r \times c$ matrix containing the turbulent phase values. The, physical dimension of each pixel in the matrix is $p_s \times p_s$.

Then, simulating new values of the turbulence is equivalent to generating new columns of the phase screen matrix and properly shifting the window corresponding to the telescope aperture. Thus, to simplify the notation, hereafter we omit the time coordinate t from equations, and we focus on the goal of generating an $r \times c$ phase screen (where c can go to infinity and r can be chosen arbitrarily large).

In this framework, the turbulent phase can be treated as a realization of a zero-mean wide-sense stationary stochastic process φ. Then, the problem of phase screen synthesis can be stated as the simulation of φ. Recently proposed methods, [1],[2],[8], perform such simulation using a properly computed linear dynamic system:

$$\begin{cases} \chi_s(u+1) = A_s\chi_s(u) + K_s\xi(u) \\ \varphi(u) = C_s\chi_s(u) + \xi(u) \end{cases} \quad (2)$$

where $\varphi(u)$ is a vector containing the values of the uth column of the synthesized turbulent phase, χ_s is the state of the linear system and ξ is a zero-mean Gaussian white-noise process.

The advantage of using (2) for turbulence simulation is twofold: It accurately reproduces the turbulence temporal dynamic and it can be used to produce infinite sequences of phase screens.

On the other hand, if n_s, the size of the state χ_s, is proportional to the number of rows, r, in the phase screen (i.e. assuming $n_s = O(r)$), then the computational complexity of generating a new column of turbulent phase values with (2) is $O(n_s^2)$. Similarly, the computational complexity for generating an $r \times c$ matrix of turbulent phase values is $O(r^2c)$.

In addition, similar considerations hold also for the computational load and memory requirements for computing the parameters of system (2).

Since in practical applications r can assume very large values, in such cases this method results to be impracticable, e.g. as long as $r \approx 1000$ or larger.

Hence, in this paper we propose a different approach, decomposing the problem of turbulence simulation in a two step procedure:

- Simulate the turbulent phase at low resolution, $r_s \times c_s$ ($r_s \ll r$, $c_s \ll c$) with (2) as in [1],[2],[8].
- Use a multiscale stochastic model to produce high resolution samples of the turbulence (taking as input the low resolution samples computed at the previous step).

Assume that each scale of the multiscale representation doubles the turbulence resolution, and that r_s is chosen independently on r, then M, the number of scales used in the multiscale model, is set as the least integer greater than or equal to $\log_2(r/r_s)$, e.g. $M(r) = \lceil \log_2(r/r_s) \rceil$ and $r \leq r_s 2^{M(r)}$. Then, the number of operations required for simulating the low resolution phase screen (associated to the high resolution $r \times c$ phase screen) with (2) is linearly proportional to $r_s^2 c_s$: Since r_s is constant and independent on r, and $c_s = c/2^M$, then the computational complexity of this part of the algorithm is $O(c)$. Notice that the second step of the procedure produces $r \times c$ phase screens, so its computational complexity is at least $O(rc)$, and hence the computational complexity of the first step is negligible.

The aim of the above two step procedure is to efficiently produce infinite sequences of phase screens while preserving the original statistical characteristics of the turbulence. Thus, the multiscale model shall be designed to be iteratively called after the use of system (2) to produce high resolution samples consistent with those previously generated.

Multiscale stochastic models have been widely studied in literature: The approach followed in this paper is similar to

those in [11],[3],[5],[9],[7]. The aim is that of computing a multiscale model which match some desired statistics.

Similarly to [5], we consider a multiscale linear decomposition of the signal: The resulting representation is formed by coefficients describing the characteristics of the phase screen at different scales. For simplicity of exposition, here we assume to use an Haar decomposition of the turbulent phase, as in Fig. 2.

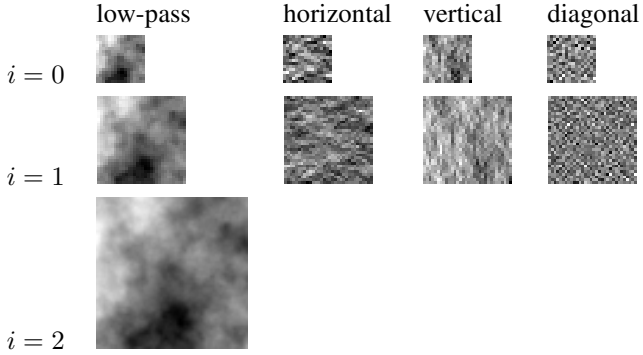

Fig. 2. Haar wavelet decomposition of a phase screen. i is the scale index, and $M=2$. The figures of the ith row represent respectively: (from left to right) the low-pass version of the current phase screen, the details on the horizontal, vertical, and diagonal direction at scale i.

Specifically, at level i of the multiscale representation the turbulent phase is decomposed in four sets of coefficients, corresponding respectively to a low-pass representation of the turbulence, and the details along the horizontal, vertical and diagonal directions (see Fig. 2). Let the order i of the representation level be larger for scales associated to higher resolution. Furthermore, let $x_i^l(u,v)$ be the low-pass coefficient at scale i and spatial position (u,v). Similarly, let $x_i^j(u,v)$, $j=\{h,v,d\}$ be the value of the coefficient for the horizontal, vertical and diagonal directions at scale i and spatial position (u,v). Let M be the scale associated to the highest resolution, then $x_M^l(u,v)=\phi(u,v),\ \forall(u,v)$. Conversely, scale 0 is the lowest resolution scale.

Then, $x_i^j(\cdot,\cdot)$, $j=\{l,h,v,d\}$ can be obtained (by means of the Haar transform) from $x_{i+1}^l(\cdot,\cdot)$ as follows:

$$\begin{bmatrix} x_i^l(u,v) \\ x_i^h(u,v) \\ x_i^v(u,v) \\ x_i^d(u,v) \end{bmatrix} = C \begin{bmatrix} x_{i+1}^l(2u,2v) \\ x_{i+1}^l(2u,2v+1) \\ x_{i+1}^l(2u+1,2v) \\ x_{i+1}^l(2u+1,2v+1) \end{bmatrix},$$

and conversely

$$\begin{bmatrix} x_{i+1}^l(2u,2v) \\ x_{i+1}^l(2u,2v+1) \\ x_{i+1}^l(2u+1,2v) \\ x_{i+1}^l(2u+1,2v+1) \end{bmatrix} = C^\top \begin{bmatrix} x_i^l(u,v) \\ x_i^h(u,v) \\ x_i^v(u,v) \\ x_i^d(u,v) \end{bmatrix},$$

where

$$C = \frac{1}{2}\begin{bmatrix} 1 & 1 & 1 & 1 \\ 1 & -1 & 1 & -1 \\ 1 & 1 & -1 & -1 \\ 1 & -1 & -1 & 1 \end{bmatrix},$$

and $C^{-1}=C^\top$.

Let x_i be the vector containing all the coefficients at scale i, i.e. $x_i^j(u,v),\ \forall(u,v),\ j=\{l,h,v,d\},\ i\neq M$, while for $i=M$ it contains $x_M^l(u,v),\ \forall(u,v)$. Then, for each i, the relation between x_{i+1} and x_i is linear and can be expressed in terms of the C matrix. In particular, recursively repeating this consideration x_i can be obtained as a linear transformation of x_M.

Furthermore, $x_M^l(u,v)=\phi(u,v),\ \forall(u,v)$, thus the second order statistics of x_M can be computed from (1). Since x_M is Gaussian, then x_i is Gaussian $\forall i\leq M$. Therefore, the second order statistics of each x_i can be derived from (1) using linear transformations.

In fact, C automatically determines the second order statistics for all $x_i,\ i\leq M$.

Thus, the goal is to define, for each i, $0\leq i<M-1$, a proper stochastic model which takes as input x_i and provides an output which matches the second order statistics of x_{i+1}. Such model will be formulated in Section IV.

Three observations are now in order: First, since the process at different scales has different statistics, the values of the parameters in model of Section IV will usually be scale dependent.

At scale 0, $x_0^l(u,v),\ \forall(u,v)$, is computed by means of the dynamic system (2). Hereafter, we assume that the parameters of system (2) are computed as described in [2] from the second order statistics of x_0^l. Alternatively, the parameters of (2) can be computed as in [1],[8]. Then, the multiscale model of Section IV will be iteratively used after that system (2) has generated one (or more) new column.

Finally, even if for simplicity of exposition the Haar transform has been used, in practice different choices may be considered. In particular, the local transformation matrix C can be scale dependent, C_i, and in some application it shall be convenient to choose it ad hoc. For instance, since usually $x_i^l(u,v)$, $x_i^h(u,v)$, $x_i^v(u,v)$, $x_i^d(u,v)$ are highly correlated, Principal Component Analysis (PCA) can be used to have a dimensional reduction on the number of coefficients to be generated at each scale.

IV. MULTISCALE STOCHASTIC MODEL

In this section we present a multiscale stochastic system which models the relation between x_{i-1} and x_i.

For simplicity of exposition we discard the border effect, that is we assume that the domain of the process at each scale is an infinite grid. Moreover, being the domains actually discrete, and $C_\phi(r)\approx 0$ for large r, then the process at each scale can be conveniently modeled as a homogeneous and isotropic Markov random field (MRF). Moreover, for simplicity of notation, in this section we consider the 1D case.

Using the 1D Haar transform, at scale i the process is formed by $\{x_i^l(\cdot)\}$ and $\{x_i^v(\cdot)\}$, where x_i^l can be computed by means of x_{i-1}: $\{x_i^l(\cdot)\}$ contains the same information of x_{i-1}, then, the aim of this section can be reformulated as statistically modeling $\{x_i^v(\cdot)\}$ given the values of $\{x_i^l(\cdot)\}$.

Let ψ be a MRF, and let the neighborhood, $\mathbb{N}(\bar{u})$, of the point u be defined as $\mathbb{N}(\bar{u})=\left\{u \mid 0<|u-\bar{u}|\leq \bar{d}\right\}$, for

a certain neighborhood size $\bar{d}$. Then, as shown in [16], the value of the MRF at the generic point $\bar{u}$, can be expressed as the best linear prediction of $\psi(\bar{u})$ given the values of its neighbors $\mathbb{N}(\bar{u})$ plus an "innovation" process $e_\psi(\bar{u})$:

$$\psi(\bar{u}) = \sum_{u \in \mathbb{N}(\bar{u})} a^{\psi}_{|\bar{u}-u|} \psi(u) + e_\psi(\bar{u}) \ , \tag{3}$$

where $\{a^{\psi}_j\}$ are suitable coefficients which yield the best (spatial) linear prediction of $\psi(\bar{u})$ given the values of its neighbors. Furthermore,

$$\mathbf{E}[e_\psi(\bar{u}) e_\psi(u)] = \begin{cases} \sigma^2_{e_\psi} & \bar{u} = u \\ -a_{|\bar{u}-u|}\sigma^2_{e_\psi} & u \in \mathbb{N}(\bar{u}) \\ 0 & \text{otherwise} \end{cases} \ . \tag{4}$$

Motivated by (3), we consider a prediction based model for x^v_i. Let $N_i(\bar{u})$ be the vector containing the following coefficients: $\{x^l_i(u)$ such that $u \in \mathbb{N}_i(\bar{u})\}$, where $\mathbb{N}_i(\bar{u}) = \left\{u \mid 0 < |u - \bar{u}| \leq \bar{d}_i\right\}$, and the size of the neighborhood, d_i, can be different at different scales.

Furthermore, let A_i be the matrix which yield to the best linear prediction of $x^v_i(\bar{u})$ given $N_i(\bar{u})$, then:

$$x^v_i(\bar{u}) = A_i N_i(\bar{u}) + e^v_i(\bar{u}) \ . \tag{5}$$

In analogy with (3), (5) can also be expressed in autoregressive-like form:

$$x^v_i(\bar{u}) = \sum_{u \in \mathbb{N}_i(\bar{u})} a^v_{i,|\bar{u}-u|} x^l_i(u) + e^v_i(\bar{u}) \ ,$$

where $\{a^v_{i,u}\}$ are the coefficients contained in A_i properly sorted.

Similarly to [7], the neat effect of using a linear (spatial) prediction is that of partially decorrelating $x^v_i(\bar{u})$ from $\{x^l_i(\cdot)\}$. In practice, the value of $\bar{d}_i$ is a design parameter which shall be chosen sufficiently large to have an effective prediction and an adequate decorrelation. On the other hand, $\bar{d}_i$ provides a bound on the computational complexity of the synthesis algorithm, then it is necessary to choose a tradeoff value of $\bar{d}_i$ to have both a good matching of the desired statistics and a sufficiently low computational complexity.

As in (4), typically $e^v_i(u)$ is not independent on $e^v_i(u')$ for $u \neq u'$. In fact, $e^v_i(\cdot)$, like x_i and x_{i-1}, is an homogeneous and isotropic random field, and $\mathbf{E}[e^v_i(\bar{u}) e^v_i(u)]$ vanishes for sufficiently large $|\bar{u} - u|$. The covariances of $e^v_i(\cdot)$ can be computed as follows:

$$\begin{aligned} \mathbf{E}[e^v_i(\bar{u}) e^v_i(u)] = \mathbf{E}[x^v_i(\bar{u}) x^v_i(u)] - A_i \mathbf{E}[x^v_i(\bar{u}) N_i(u)] \\ - A_i \mathbf{E}[N_i(\bar{u}) x^v_i(u)] + A_i \mathbf{E}[N_i(\bar{u}) N_i(u)^\top] A_i^\top \end{aligned} \tag{6}$$

where the values of the expectations can be easily obtained from the covariances of x_i.

Let $\mathcal{R}_{e,i}(r,u) = \mathbf{E}[e^v_i(u+r) e^v_i(u)]$. In fact, $\mathcal{R}_{e,i}(r,u)$ does not depend on u, then hereafter we omit to write the u: $\mathcal{R}_{e,i}(r,u) = \mathcal{R}_{e,i}(r)$. Moreover, it is simple to prove that $\mathcal{R}_{e,i}(r) = \mathcal{R}_{e,i}(-r)$.

Hereafter it is assumed that the spatial correlations of the process e^v_i can be expressed as the convolution product of a kernel and itself but considered in reverse order. When this is not the case, then if the domain of the kernel is sufficiently large, such approximation typically leads to small errors because $\mathcal{R}_{e,i}(r)$ vanishes quite fast as r becomes large. Then, the process e^v_i can be conveniently modeled as a moving average (MA) process:

$$e^v_i(u) = \sum_{k \in \bar{\mathbb{N}}} (u) \theta_{i,k} \epsilon_i(u-k) \ , \tag{7}$$

where ϵ_i is a zero-mean Gaussian white-noise process, $\bar{\mathbb{N}}(u)$ is a suitable neighborhood of u, and $\{\theta_{i,\cdot}\}$ are the MA coefficients.

The computation of proper values of the parameters $\{\theta_{i,\cdot}\}$ to make the covariances of the MA process match those in (6) is a problem already investigated in literature (it is equivalent to the minimum length correlation extension problem). The problem can be solved as in [15] finding the sequence $\{\theta_{i,\cdot}\}$ of minimal length ensuring the match. However, the method presented in [15] is quite laborious in the multidimensional case, hence we proceed in a different way. Assume to have considered a neighborhood $\bar{\mathbb{N}}(\cdot)$ which is sufficiently large to contain the domain of the coefficients $\{\theta_{i,\cdot}\}$. Then, they can be computed very quickly as follows [10]:

- Let $\mathbf{r_e}$ be a vector containing the finite symmetric covariance sequence of $\mathcal{R}_{e,i}(\cdot) \neq 0$.
- $\mathbf{r_e}$ is formed by the covariances of $e^v_i(\cdot)$ in (7), then $\mathbf{r_e} = \mathbf{g} * \bar{\mathbf{g}}$, where $\mathbf{g}$ is a vector containing the MA coefficients $\{\theta_{i,\cdot}\}$, and $\bar{\mathbf{g}}$ contains the same coefficients of $\mathbf{g}$ but in reverse order.
- Let $\mathcal{F}(\mathbf{g})$ be the fast Fourier transform (FFT) of $\mathbf{g}$. Then, from the convolution property of the FFT: $\mathcal{F}(\mathbf{g} * \bar{\mathbf{g}}) = \mathcal{F}(\mathbf{g}) \cdot \mathcal{F}(\mathbf{g})$, where in the last equation "$\cdot$" indicates the element by element multiplication.
- Since $\mathcal{R}_{e,i}(\cdot)$ is even and real, then $\mathbf{r_e}$ and $\mathcal{F}(\mathbf{r_e})$ are symmetric and real vectors.
- From the above considerations: $\mathcal{F}(\mathbf{r_e}) = \mathcal{F}(\mathbf{g} * \bar{\mathbf{g}}) = \mathcal{F}(\mathbf{g}) \cdot \mathcal{F}(\mathbf{g})$.
- From the properties of stationary processes it is simple to prove that each component of the vector $\mathcal{F}(\mathbf{r_e})$ is positive.
- Finally, each component of $\mathcal{F}(\mathbf{g})$ is obtained taking the square root of the corresponding component in $\mathcal{F}(\mathbf{r_e})$, and $\mathbf{g}$ (and consequently $\{\theta_{i,\cdot}\}$) is obtained computing the inverse FFT of $\mathcal{F}(\mathbf{g})$.

The above procedure does not necessarily lead to the optimal set of parameters (the minimum length sequence which reproduces the desired covariances), however it quickly provides a solution.

Then, the synthesis procedure iteratively executes the following steps:

1) System (2) produces new low-resolution samples, $\{x^l_0(u)\}_{u=u_1:u_2}$.
2) for $i = 0 : M-1$
   - use A_i to compute predictions $\{\hat{x}^v_i(u)\}_{u=u_1:u_2}$ of the new values of $\{x^v_i(u)\}_{u=u_1:u_2}$ based on $\{x^l_i(u)\}_{u=1:u_2}$.

- generate new values of $\epsilon_i(\cdot)$ sampling from a zero-mean white-noise random generator.
- compute $\{e_i^v(u)\}_{u=u_1:u_2}$ filtering $\epsilon_i(\cdot)$.
- compute the details at scale i, as

$$x_i^v(u) = \hat{x}_i^v(u) + e_i^v(u),\ u = u_1 : u_2\ ,$$

and combine $\{x_i^v(u)\}_{u=u_1:u_2}$ with $\{x_0^l(u)\}_{u=u_1:u_2}$ to obtain $\{x_{i+1}^l(u)\}_{u=2u_1:2u_2+1}$.

end

3) $\phi(u) = x_M^l(u),\ \forall u$.

The above procedure can be adapted to the 2D case with minor changes. The main computational cost of the algorithm is due to filtering operations. Since the number of coefficients in the Haar description of the phase screen is equal to the size of the phase screen itself, and since the dimensions of the neighborhood $\{\mathbb{N}_i\}$ and $\{\bar{\mathbb{N}}_i\}$ do not depend on r and c, then, the number of operations needed for generating an $r \times c$ matrix of turbulent phases is $O(rc)$.

V. SIMULATIONS AND DISCUSSION

In this section we investigate the performances of the proposed method in a case of study: We simulate the atmospheric turbulence for a telescope with diameter $d = 8$ meter, and we set $L_0 = 50$m, $r_0 = 0.2$m. Specifically, we generate a 3840×3840 pixels phase screen corresponding to a 8×8 m^2 area, as shown in Fig. 3 (bottom).

Without loss of generality, as in Section III we have assumed that the wind direction is parallel to $\mathbf{v}$. Then, we have simulated the turbulence at low resolution, $r_s \times c_s$, as described in [2], setting $r_s = 60$, and consequently $M = 6$ (so $3840 = 2^M r_s$). In this simulation $c_s = 60$, however the method described in this paper can generate infinitely long sequences of columns, hence the turbulence can be simulated for whatever choice of c and c_s. The low resolution generated phase screen is shown at the top of Fig. 3.

The neighborhood size, $\bar{d}_i$, for (5) is set to 5 for each $i = 0, \ldots, M$. Furthermore, the prediction error in (5), modeled as in (7), has only local covariances different from zero, i.e. $\mathcal{R}_{e,i}(r)$ vanishes quickly as r becomes larger, then we set $\bar{\mathbb{N}}_i(u, v) = \mathbb{N}_i(u, v)$.

The multiscale model of Section IV generates the high resolution phase screen, bottom of Fig. 3, retaining the low spatial frequencies characteristics computed with [2] however adding high spatial frequencies details. To make clear the effect of the multiscale model, in Fig. 4 we zoom on a 2.1×2.1 m^2 window of Fig. 3 and we compare the generated phase screen at low (scale 0) and the high (scale $M = 6$) resolution. Notice that the pixel dimension at low resolution is 0.13×0.13m, while at high resolution it is $p_s \times p_s$, where $p_s \simeq 0.0021$m.

In Fig. 5 we compare the statistics of the generated phase screen with the theoretical ones: Astronomers commonly describe the turbulent phase spatial statical characteristics by means of the structure function, $D_\phi(\cdot)$, which can be computed as:

$$D_\phi(r) = 2(C_\phi(0) - C_\phi(r))\ . \tag{8}$$

Fig. 5 compares the sample estimates of the structure function, obtained from a synthesized phase screen, with those computed by means of (8). As shown in [2], it is more difficult for methods based on (2) to correctly reproduce the structure function along the wind direction than along its orthogonal direction: Then, in Fig. 5 we compare the structure functions along the wind direction.

We stress the fact that the sample structure function in Fig. 5 has been estimated using just a 960×960 phase screen: Despite the estimates are obtained using a relatively small number of correlated phase samples, they are close to the theoretical structure function values.

It is worth to notice that while in Section IV we have discarded the border effect, in practical applications this has to be handled: This can be easily done for instance simulating the turbulence on an oversized area and then discarding the additional points on the borders.

To conclude, we examine the proposed synthesis algorithm from a computational point of view. Since the dimension of telescopes is ever growing, and an accurate spatial description of the values of the turbulence phase allows to more precise evaluations of the AO system performances, then in the following we derive the computational complexity of the overall algorithm in generating a long sequence of high resolution phase screens (i.e. r is large and c goes to infinity) with respect to both r and c. Since the value of r_s is fixed, then, as shown in Section III, the computational complexity of generating the $r_s \times c_s$ low resolution phase screen with (2) is $O(c)$. On the other hand, the synthesis of the multiscale coefficients is $O(rc)$ (Section IV), thus the overall computational complexity of the algorithm is $O(rc)$. Thus, the proposed approach significantly reduces the computational load of (2) (which is approximatively $O(r^2 c)$, Section III) for the synthesis of high resolution phase screens.

Similar considerations can be repeated for the problem of computing the parameters of the multiscale model: At each scale the computation of the parameters of (5) and (7) involve the use of only local statistics, thus without requiring large amounts of memory nor of time.

VI. CONCLUSIONS

In this paper we have proposed a new method for simulating high resolution phase screens. Such method is based on the combination of a dynamic system [2],[1],[8], which simulates the low-resolution temporal dynamic of the turbulence, with a multiscale stochastic model, which generates the high-resolution details of the turbulent phase.

The resulting procedure, which can be used for simulating infinite sequences of turbulent phases, ensures that the generated samples reproduce with high accuracy the theoretical statistics of the turbulence.

On the other hand, the overall computational complexity of the synthesis procedure is particularly appealing thanks to the great ability of multiscale models to capture the turbulence spatial statistical characteristics in a compact and efficient representation.

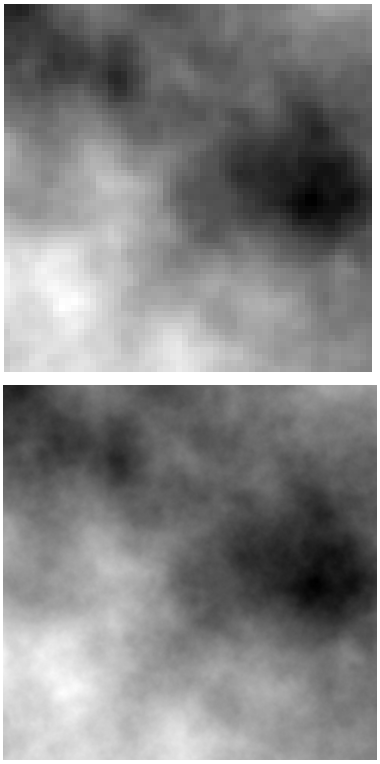

Fig. 3. Phase screen synthesis, 8×8 m^2 window: (top) low resolution x_0^l, 60×60 pixels, and (bottom) high resolution x_6^l, 3840×3840 pixels.

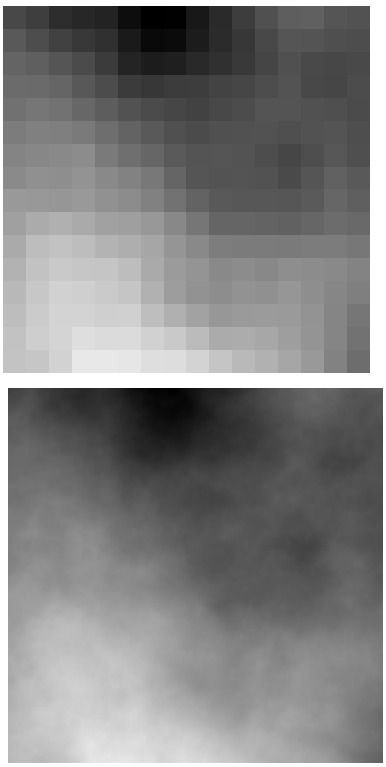

Fig. 4. Phase screen synthesis, zoom on a 2.1×2.1 m^2 window: (top) low resolution x_0^l, 16×16 pixels, and (bottom) high resolution x_6^l, 1024×1024 pixels.

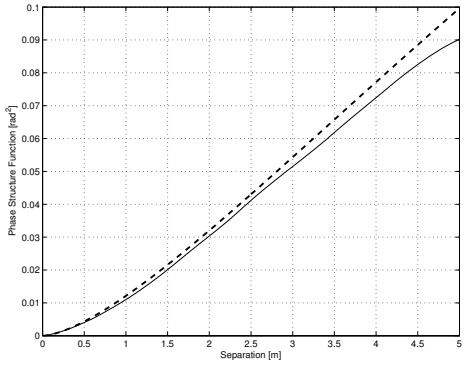

Fig. 5. Comparison of the theoretical structure function (bold-dashed line) with the sample structure function (solid line) evaluated along the wind direction computed from a 960×960 phase screen.

REFERENCES

[1] F. Assemat, R.W. Wilson, and E. Gendron. Method for simulating infinitely long and non stationary phase screens with optimized memory storage. *Optic express*, 14(3):988–999, February 2006.

[2] A. Beghi, A. Cenedese, and A. Masiero. Stochastic realization appoach to the efficient simulation of phase screens. *Journal of the Optical Society of America A*, 25(2):515–525, February 2008.

[3] A. Benveniste, R. Nikoukhah, and A.S. Willsky. Multiscale system theory. *Circuits and Systems I: Fundamental Theory and Applications, IEEE Transactions on*, 41(1):2 –15, jan 1994.

[4] R. Conan. *Modelisation des effets de l'echelle externe de coherence spatiale du front d'onde pour l'observation a haute resolution angulaire en astronomie*. PhD thesis, Univ. Nice Sophia Antipolis, 2000.

[5] K. Daoudi, A.B. Frakt, and A.S. Willsky. Multiscale autoregressive models and wavelets. *Information Theory, IEEE Transactions on*, 45(3):828 –845, apr 1999.

[6] I. Daubechies. *Ten Lectures on Wavelets*. CBMS-NSF Lecture Notes nr. 61, SIAM, 1992.

[7] A.B. Frakt and A.S. Willsky. Computationally efficient stochastic realization for internal multiscale autoregressive models. *Multidimensional Syst. Signal Process.*, 12(2):109–142, 2001.

[8] D.L. Fried and T. Clark. Extruding kolmogorov-type phase screen ribbons. *Journal of the Optical Society of America A*, 25(2):463–468, February 2008.

[9] W.W. Irving and A.S. Willsky. A canonical correlations approach to multiscale stochastic realization. *Automatic Control, IEEE Transactions on*, 46(10):1514 –1528, oct 2001.

[10] M. Le Ravalec, B. Noetinger, and L.Y. Hu. The fft moving average (fft-ma) generator: An efficient numerical method for generating and conditioning gaussian simulations. *Mathematical Geology*, 32(6):701–723, aug 2000.

[11] M.R. Luettgen, W.C. Karl, A.S. Willsky, and R.R. Tenney. Multiscale representations of markov random fields. *Signal Processing, IEEE Transactions on*, 41(12):3377 –3396, dec 1993.

[12] S. Mallat. *A Wavelet Tour of Signal Processing*. Academic Press, 1999.

[13] F. Roddier. The effects of atmospheric turbulence in optical astronomy. *Progress in Optics*, 19:281–376, 1981.

[14] F. Roddier. *Adaptive optics in astronomy*. Cambridge univ.press, 1999.

[15] A.O. Steinhardt. Correlation matching by finite length sequences. *Acoustics, Speech and Signal Processing, IEEE Transactions on*, 36(4):545–559, apr 1988.

[16] J.W. Woods. Two-dimensional discrete markovian fields. *IEEE Trans. on Information Theory*, 18(2):232–240, 1972.